Modeling Heat and Degree of Gelation for Methyl Cellulose Hydrogels with NaCl Additives

S. C. Joshi, Y. C. Lam

School of Mechanical and Aerospace Engineering, Nanyang Technological University, Singapore, 639 798, Singapore

Received 25 April 2005; accepted 18 October 2005
DOI 10.1002/app.23565
Published online in Wiley InterScience (www.interscience.wiley.com).

ABSTRACT: Methyl cellulose (MC) hydrogels are thermoreversible physical hydrogels and their gelation is an endothermic process. A model consisting of a generalized expression for two bell-shape curves was formulated to describe and capture enthalpy changes that take place during the gelation of an aqueous solution of MC, SM4000, in the presence of sodium chloride, NaCl, in different concentrations. The procedure followed in obtaining the necessary constants for the model using the differential scanning calorimetric (DSC) measurements is elaborated. The developed model described the salt-out effects of NaCl in various % on the MC gelation very well. One of the two bell-shape curves mapped most part of the DSC thermograms. The secondary bell-shape curves portrayed the minor enthalpy changes. The possible mechanisms and molecular bonding processes driven by the energy represented by the area under these two individual curves are discussed. Subsequently, a sigmoidal growth model for the degree of gelation was introduced, and its development is explained in the paper. The import of various constants for these two models, the bell-shape curves and the sigmoidal growth models, in terms of gelation kinetics is identified. The need for a specific term of the sigmoidal model for depicting the effect of the salt additive onto the gelation is recognized. The comparison between the results obtained using these two models is discussed. © 2006 Wiley Periodicals, Inc. J Appl Polym Sci 101: 1620–1629, 2006

Key words: methyl cellulose; hydrogels; gelation; differential scanning calorimeter (DSC); sigmiodal model; salt additives

INTRODUCTION

Hydrogels are crosslinked networks of hydrophilic/hydrophobic polymers, which are formed either by chemical or physical bonds in water. They possess the ability to absorb large amounts of water and swell while maintaining their three-dimensional structure.

Hydrogels are increasingly being used in biomedical, food, and pharmaceutical industries. Most hydrogels undergo transformation from solution to gel form (commonly termed as gelation process) upon either cooling or heating. Such thermosensitive hydrogels are gaining more importance and being explored as media for controlled drug release.[1–4]

Methyl cellulose (MC), which is extensively used as a thickener or binder in pharmaceutical, ceramic processing, and food applications, undergoes gelation in aqueous solution upon heating.[5–7] Gelation of MC has been a key area of research, and a clear and complete picture of the gelation mechanism has not yet been established. The sol–gel transformation process for MC, as illustrated in Figure 1, is based on various explanations provided by other researchers[5–9] and our earlier studies.[10] According to Kobayashi et al.,[8] at low temperatures, because of the polar nature, water molecules surround the hydrophobic methoxyl groups of MC, forming cages so that MC becomes water-soluble [Fig. 1(a)]. However, upon heating, these surrounding water structures deform and break to expose the hydrophobic regions of MC [Fig. 1(b)]. Because of the hydrophobic nature of these side groups, the MC chains in the aqueous solution move towards each other, bringing side groups together to associate and form aggregates or interchain clusters [Fig. 1(c)]. As temperature rises further, more and more hydrophobic aggregates are formed. Eventually, these aggregates join together through the hydrophobic groups, developing into a three-dimensional physical network of MC chains [Fig. 1(d–f)]. Even when the network is fully developed, the MC mers are still in relaxed state, rendering the network cells flexible. Gradually, as the temperature increases, the water uptake and entrapment of water molecules into these network cells increase, resulting in enlargement of these cells to full-size, reducing their flexibility [Fig. 1(g–h)]. The continued swelling of the network of MC chains is due to the osmotic forces, which are opposed by the elastic retraction forces of the network. Eventually, an equilibrium swelling level is attained,[11] resulting in a fully developed and stabilized MC gel [Fig. 1(i)].

Correspondence to: S. C. Joshi (mscjoshi@ntu.edu.sg).

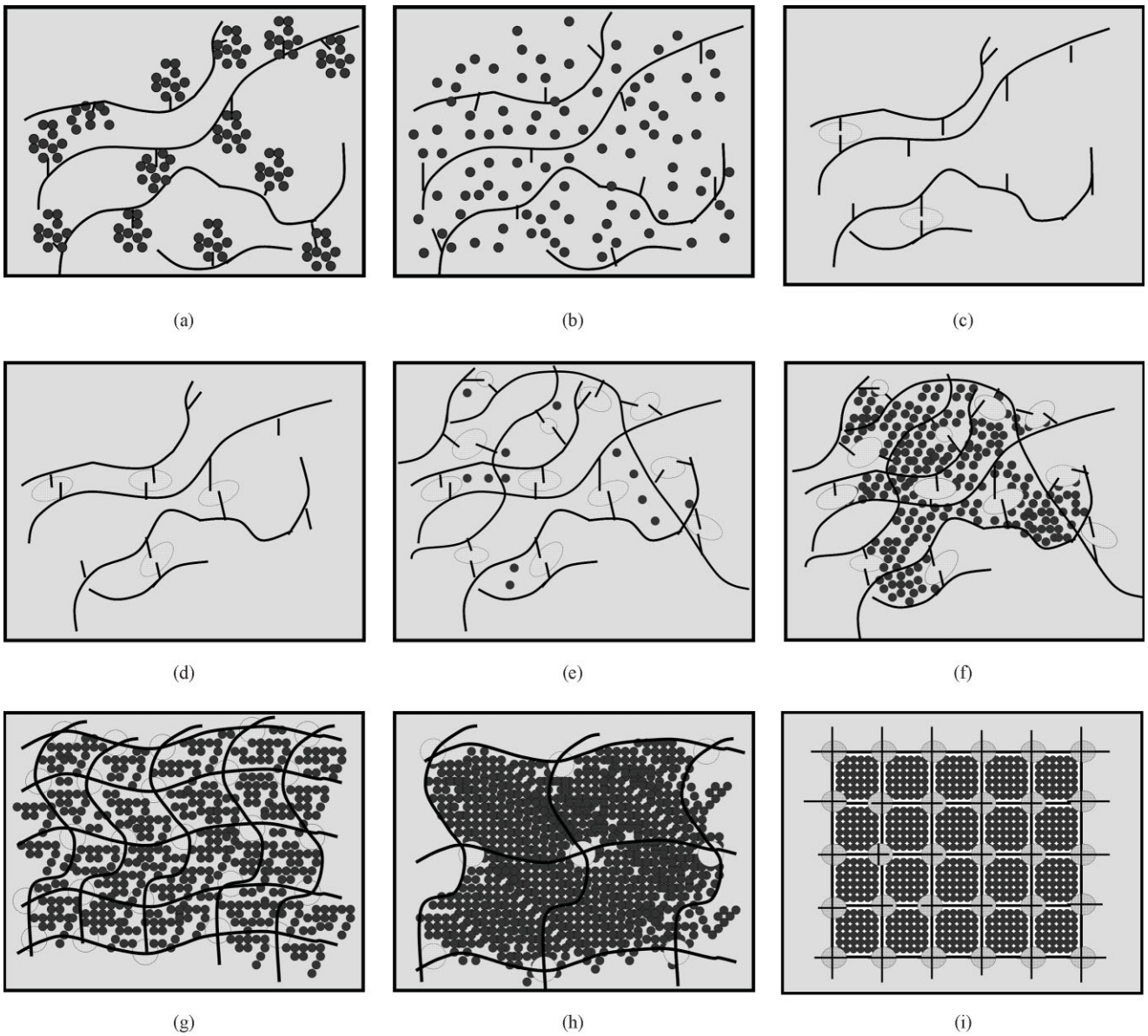

Figure 1 Schematic illustration of temperature dependent sol–gel transformations for aqueous solution of MC. Black dots represent water molecules. Dark lines are the MC chains with the short branches as methoxyl side groups. Hydrophobic associative bonds of these side groups are shown on a patterned whitish oval shapes. (a) Water cages surrounding methoxyl groups, (b) melting of water cages, (c) MC macromolecules coming closer, (d) hydrophobic association, (e) network formation in progress, (f) entrapment of water molecules, (g) increased water uptake, (h) enlargement of network cells, (i) fully developed and stabilized gel. [Color figure can be viewed in the online issue, which is available at www.interscience.wiley.com.]

As such, the sol–gel transformation of MC in an aqueous solution is distinctively marked by two processes namely, the formation of MC chain network and the swelling or expansion of the various cells in the network, resulting into a fully developed gel. Both these transformations are linked to the absorption and utilization of heat energy, generally referred to as the heat of gelation. Differential scanning calorimeter (DSC) measurements have been successfully used to obtain quantitative information about the heat of gelation.[6,9,12]

Kundu and Kundu[13] investigated the effect of sodium chloride, NaCl, when added to aqueous solutions of MC, with the MC content below 1%, on the DSC measurements. It was observed that the temperature at which absorption of heat was at the peak decreased with increase in the salt concentration. This is an important salt-out phenomenon that can be used to alter the sol–gel transition process to suit a particular application. Xu et al.[14,15] also carried out DSC measurements on MC solutions in the presence of NaCl to understand the salt-out mechanism further.

Newer inventions are seen where MC is modified to match their salt-out effects at body temperature.[16]

The current work focuses on the modeling of the changes in enthalpy associated with the gel formation process for MC with NaCl additives at different concentration. Unless such models are available, various applications of MC hydrogels, including drug delivery and drug release, cannot be systematically analyzed, understood, and improved. In our earlier work,[10] a generalized formulation was developed and validated for modeling MC gelation. In this work, the same formulation is modified and extended further to capture the salt effects. The necessary parameters in the formulation were determined such that a close agreement was established with the DSC heating thermograms. During the model formation, it was noticed that more than one bell-shape curves, one major and one minor, were necessary to depict the enthalpy changes adequately. It was hypothesized that the major curve was related to a major enthalpy change associated with the movement of MC chains, the formation of MC aggregates, and the hydrophobic association of MC groups, finally leading to the development of a three-dimensional gel network and its subsequent swelling. The term swelling is used to highlight the enlargement of MC network cells because of uptake and entrapment of water molecules in them. The minor curve was associated with a minor enthalpy change primarily involving the ionic interaction of the salt with water, the water-to-water and the water-to-polymer hydrogen bonding, and the energy associated in stabilizing the swollen gel network. Subsequently, an analytical model for the degree of gelation was introduced and its development discussed for studying the effects of various concentrations of NaCl on the gelation of MC further.

MATERIALS AND EXPERIMENTAL DATA

The DSC data, i.e., the relative thermal capacity, C_p, was acquired[14,15] using a microdifferential scanning calorimeter (VP-μDSC, MicroCal) for the aqueous solutions of 0.03 m*M* (0.93 wt %) of MC with different % of NaCl, namely 0.2*M*, 0.4*M*, 0.6*M*, and 0.8*M*. Deionized water was taken as a reference during the heating process at the rate of 1°C/min. Methylcellulose (MC), with the trade name SM4000, was provided by Shin-Etsu Chemical Co. It has a weight–average molecular weight (M_w) of 310,000 g/mol and an average degree of substitution (DS) of 1.8. NaCl was purchased from Sino Chemical Co. (Pte).

The DSC results for the MC–NaCl solutions as documented and discussed in Refs. 14,15 were used in the current work to demonstrate the development and validity of the models. These DSC results were obtained at a constant heating rate of 1 °C/min without any isothermal hold in between, and no observation about phase separation was reported. It was observed that the baseline C_p values in all cases showed small fluctuations around zero because of the initial unsteady state of the solutions and the temperature conditions before the DSC measurements attained a steady trend. As the magnitude of the C_p value at the base was insignificant, its small fluctuation would have little effect on the enthalpy calculations. As such, for convenience, a single base C_p value of 1×10^{-4} kJ/mol/°C was used to normalize the experimental data as depicted in Figure 2. The plots indicated that the addition of salt had an effect on the onset (T_{on}), the peak (T_p), and the offset (T_{off}) temperatures for the sol–gel transformations.

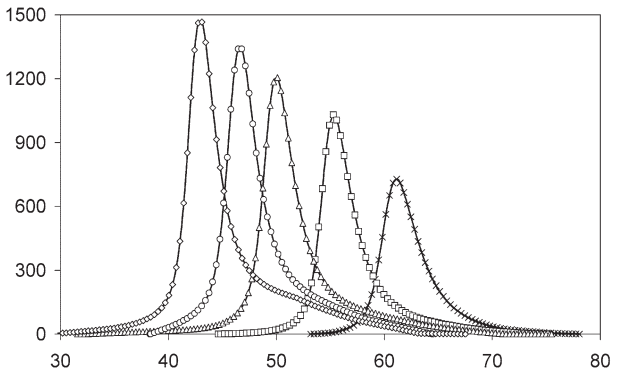

Figure 2 DSC curves for different NaCl concentrations in 0.03 mM (0.93 wt %) of MC solutions (scanning rate 1°C/min). X axis, temperature (°C); Y axis, experimental C_p (common baseline) (kJ/mol/°C). ×, without salt; □, 0.2*M* of salt; △, 0.4*M* of salt; ○, 0.6*M* of salt; and ◇, 0.8*M* of salt.

Model development and implementation

It was observed that most of the heating thermograms for gelation of MC hydrogels were unsymmetrical and bell-shaped (Fig. 2), which required a generalized mathematical formulation to represent them. One such formulation [eq. (1)] was established earlier by the authors:[10]

$$C_p(T - T_p) = \frac{\mathrm{NR}}{\mathrm{DR}_1 + \mathrm{DR}_2} = \frac{(\lambda_1 + \lambda_2)C_{p\max}}{\lambda_1 e^{(T-T_p)C_1} + \lambda_2 e^{-(T-T_p)C_2}} \quad (1)$$

where $C_p(T - T_p)$ refers to the thermal function of the specific heat capacity, NR signifies the numerator term, and DR1 and DR2 designate part 1 and part 2 of the denominator. λ_1, λ_2, C_1, and C_2 are the empirical constants, which are to be determined by minimizing the discrepancy between the experimental data (DSC thermogram) and the mathematical formulation [eq. (1)].

There are a few similarities in the thermal behavior of hydrogels[10] and other polymers.[17,18] Crystallization

of thermoplastics, curing of thermosetting resins, and gelation of hydrogels are all governed by thermodynamic considerations. Crystallization and curing are exothermic reactions, whereas gelation, depending on the type of hydrogel, can be either endothermic or exothermic process. Both crystallization and physical gelation are thermoreversible processes. Thermosetting resins and hydrogels both have three-dimensional networks. Therefore, the term "degree of gelation " (α_g), similar to the degree of cure or the degree of crystallization, was introduced for quantitative assessment of the state of gelation.[10] Once the DSC data is mapped, α_g at any temperature T can be calculated as

$$\alpha_g = \frac{\text{Heat absorbed upto a stage}}{\text{Heat for complete gelation}} = \frac{H}{H_T} = \frac{\int_{T_{on}}^{T} f(T)dT}{\int_{T_{on}}^{T_{off}} f(T)dT} \quad (2)$$

Note that α_g is a fraction that varies from 0 to 1 and is dimensionless. α_g =0 at $T = T_{on}$ and when $T = T_{off}$, α_g = 1. Equations (1) and (2) were successfully used to describe the DSC heating thermograms and to obtain the heat and the degree of gelation for MC solutions of different concentrations without any additives.[10] The significance of the various constants was yet to be elaborated and will now be discussed.

From eq. (1), NR is a multiplier that is determined based on the scaling requirement for 1/(DR1+DR2). The denominator terms control the spread and the shape of the C_p curve. DR1 describes the decaying arm of the curve between T_p and T_{off} whereas DR2 maps the growing arm from T_{on} to T_p. Both, DR1 and DR2, have a form similar to the Arrhenius equation[19] describing the progress of a reaction as a function of temperature with time. Thus the associated constants could have similar significance. λ_1 and λ_2 are the frequency parameters with the unit 1/°C. The terms C_1 and C_2 resemble $R/\Delta E$ term, where ΔE is the activation energy (J/mol) and R the universal gas constant (8.314 J/mol K). Since gelation takes place only within a certain temperature window when the temperature is allowed to increase at a certain rate, the temperature difference holds the key for the reaction. Under isothermal conditions or at slow rate of heating, the gelation process appears to attain equilibrium rapidly, with no further change in the state of gelation. This suggests that for a reasonably slow scan rate of 1°C/min, the temperature difference and not the duration of the temperature change is the important parameter for gelation modeling. It was, therefore, possible to establish a model based on the usual temperature unit (°C). The units for C_1 and C_2 in the current case thus remain as 1/°C, which cancel out with the temperature units for $(T - T_p)$ terms. DR1 and DR2 will have the same unit as the λ terms. Finally, $C_p(T - T_p)$ would have the same unit as that of C_{pmax} (J/mol °C) as required.

Equations (1) and (2) were first used to describe the C_p curves and α_g for MC solutions with 0.2M and 0.8M NaCl. The comparison between the model and the experimental data are shown in Figure 3. It is observed from these plots that the basic model, namely eq. (1), cannot describe the process well around the shoulders of the C_p curves. Rather large discrepancies between the model and the experimental data manifested themselves at the beginning and towards the end of gelation. These differences were reflected in the degree of gelation curves also. It is observed that the discrepancies increased with the increasing NaCl concentration. Thus the model, which reasonably predicted the gelation process for MC without salt, was unable to describe the heat absorption mechanism successfully for the sol–gel transformations in the aqueous solution of MC in the presence of NaCl.

These discrepancies suggest that there are additional mechanisms taking place because of the addition of NaCl. By hypothesizing that these additional mechanisms follow a similar trend for the rate of energy absorption and that the effects of more than one binding process and mechanism can be superimposed, an expression similar to eq. (1) can be added to describe these mechanisms. Thus, to account for the effects of the salt additive, a model that consisted of two expressions, with each part similar to that of eq. (1), was employed; see eq. (3).

$$C_p(T - T_p) = \frac{(\lambda_1 + \lambda_2)C_{pv1}}{\lambda_1 e^{(T-T_{p1})C1} + \lambda_2 e^{-(T-T_{p1})C2}} + \frac{(\lambda_3 + \lambda_4)C_{pv2}}{\lambda_3 e^{(T-T_{p2})C3} + \lambda_4 e^{-(T-T_{p2})C4}} \quad (3)$$

where λ_1, λ_2, λ_3, λ_4, C_1, C_2, C_3 and C_4 are the empirical constants. Note that parameters C_{pmax} and T_p used in eq. (1) are replaced by C_{pv1}, T_{p1}, C_{pv2}, and T_{p2} in eq. (3). This bi-expression model was expected to provide two bell-shape curves, which when superimposed would closely follow the experimental DSC curves.

The constants for the equation could be determined by minimizing the discrepancies between the model [eq. (3)] and the experimental data. The least square technique was adopted in which the values for the constants were obtained by iteratively minimizing the sum of the square of errors in C_p values calculated as

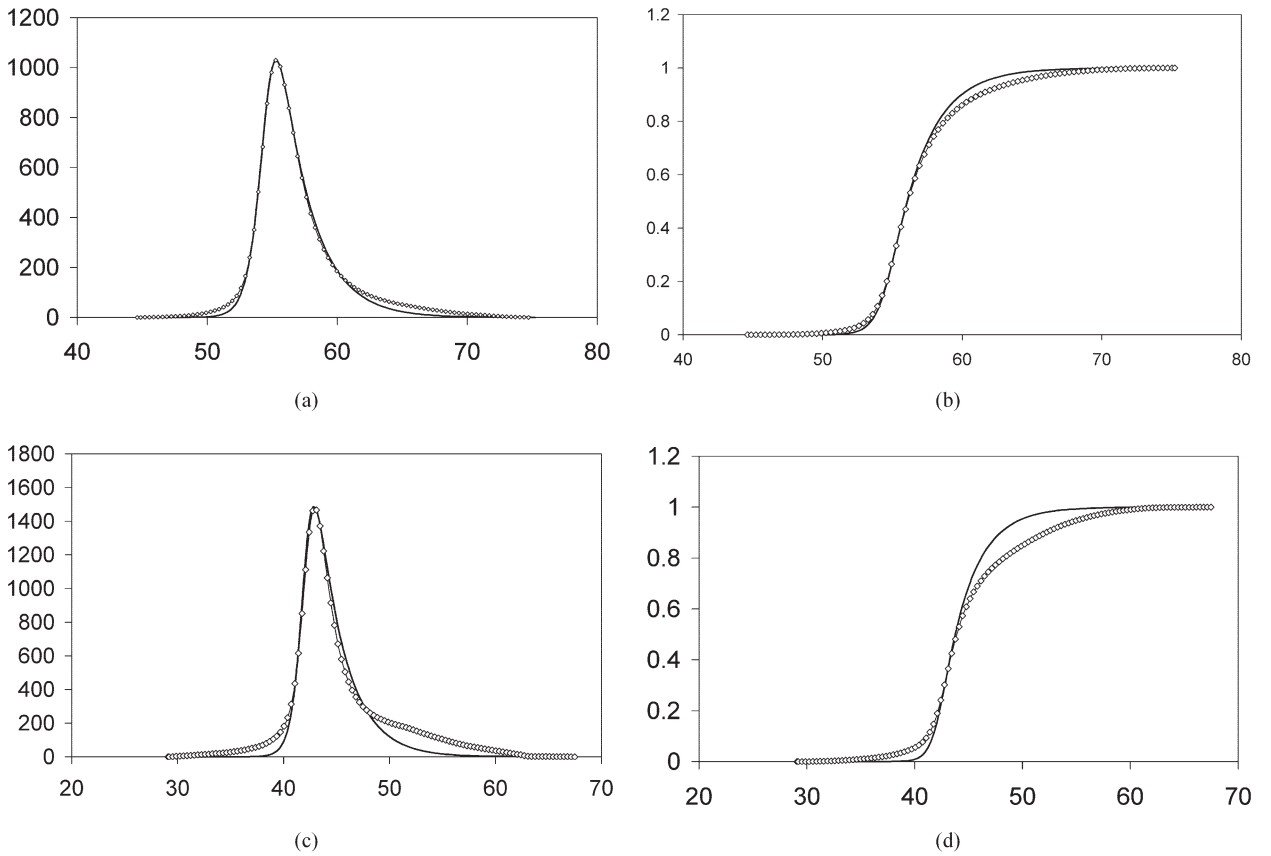

Figure 3 Specific heat capacity and degree of gelation curves for MC hydrogel with NaCl (the single bell-shape model). Heating of MC with (a) 0.2*M* and (c) 0.8*M* of NaCl. X axis, temperature (°C); Y axis, relative C_p (kJ/mol/°C). ◇, normalized DSC data; –, C_p model [eq. (1)]. Degree of gelation with (b) 0.2*M* and (d) 0.8*M* of NaCl. X axis, temperature (°C); Y axis, degree of gelation. ◇, experimental data; –, model [eqs. (1) and (2)].

$$\sum_{i=1}^{N}[C_{p(\text{expt})} - (C_{p1(\text{model})} + C_{p2(\text{model})})]^2 \rightarrow 0 \qquad (4)$$

where, $i = 1$ at $T = T_{\text{on}}$ and $i = N$ when $T = T_{\text{off}}$. This generated two bell-shape curves with C_{pv1} and C_{pv2} as their respective peak C_p values.

RESULTS AND DISCUSSIONS

Figure 4 shows the heat capacity curves obtained using the new model [eq. (3)] and its comparison with the DSC thermogram data for different concentrations of NaCl. The derived empirical constants for the model are listed in Table I.

As NaCl is an electrolyte, the Cl^- ions compete with the MC chains for hydrogen (H) bonding with water molecules.[14] In addition, polar natured water molecules form cages around the Na^+ ions. There is also a likelihood of chloride–MC bonds. These collectively promote early exposure of the hydrophobic groups and the formation of MC aggregates at lower temperature. As a result, T_p for MC gels decreases with an increase in the NaCl concentration.

All the C_p curves exhibited a trend that the dominant or the major bell-shape curve was always able to map most of the experimental data and was designated as the primary curve. The secondary curve, which always appeared small, however, was necessary to provide good fit to the left- and right-hand shoulders of the curve. As mentioned earlier, the low temperature activities are dominated by water-to-water and water-to-MC hydrogen bonding. The low-magnitude, initial portion of the primary curve describes the energy consumption causing disruption in these bonding processes. In a similar manner and in small magnitude also, the ionic interaction of salts with water, which is also through H bonding, is represented by the initial portion of the secondary curve. This reflects that such H bonding does not involve substantial amount of energy.

Following the breakage of water-cages surrounding the hydrophobic side groups of MC chains, the MC chains tend to move towards each other for association. However, these macromolecules of MC are considerably long in comparison with the molecules of NaCl and H_2O. It is expected that a substantial amount of energy is required to facilitate their move-

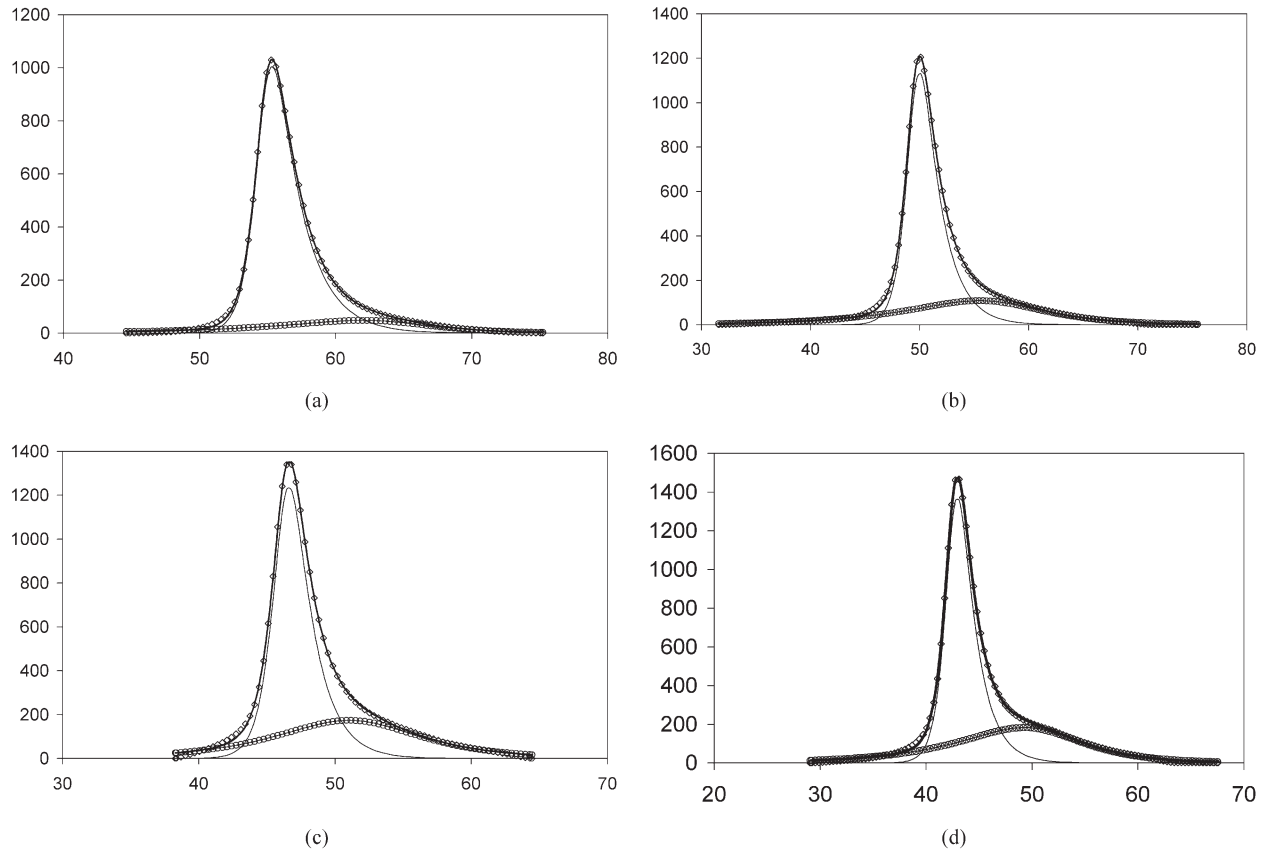

Figure 4 Specific heat capacity curves for the MC hydrogel with NaCl (the two bell-shape model). Heating of MC with (a) 0.2*M*, (b) 0.4*M*, (c) 0.6*M*, and (d) 0.8*M* of NaCl. X axis, temperature (°C); Y axis, relative C_p (kJ/mol/°C). ◇, normalized DSC data; —-, modeled C_{p1}; ○, modeled C_{p2}; –, modeled total C_p.

ment in the solution. This justifies the substantial and fast rise in the C_p values. As the MC molecules come closer, they start to form groups through a few hydrophobic bonds. These groups further join together and start to form a network. This initial phase of hydrophobic association is referred to as noncooperative association and requires more energy as compared to the subsequent bonding. The subsequent hydrophobic association occurs among the already connected MC chains, thereby increasing the density of the network cells. This type of bonding requires much less energy and is called as cooperative association. As long as the process of noncooperative association goes on, the energy absorption continues at a high rate, marked by

TABLE I
The Model Constants for C_p Curves [eq. (1) and (3)]

Constants	NaCl concentration				
	0.0*M* (eq. 1)	0.2*M* (eq. 3)	0.4*M* (eq. 3)	0.6*M* (eq. 3)	0.8*M* (eq. 3)
λ_1 (1/°C)	1.8985	1.9774	2.9376	0.0402	4.6263
λ_2 (1/°C)	0.632	2.2097	1.3632	0.00952	0.3665
λ_3 (1/°C)	—	0.0971	0.0737	0.3072	0.0975
λ_4 (1/°C)	—	0.1256	0.1262	0.8208	1.435
C_1 (1/°C)	0.392	0.4882	0.5532	0.6232	0.6091
C_2 (1/°C)	1.144	1.3319	1.2516	1.2024	1.2837
C_3 (1/°C)	—	0.2961	0.2228	0.2292	0.2397
C_4 (1/°C)	—	0.1428	0.1448	0.1998	0.1560
C_{pv1} (kJ/mol/°C)	—	874.2	1134.47	1164.78	1054.95
C_{pv2} (kJ/mol/°C)	—	47.074	108.539	160.079	115.996
T_{p1} (°C)	61.14	54.71	49.96	47.04	43.88
T_{p2} (°C)	—	63.11	55.18	49.07	43.53

the C_p reaching its peak C_{pv1}. It is anticipated that the cooperative association will go on for some more time until the network develops into a full three-dimensional structure. However, this stage has a much subsided energy requirement and the C_p values start to recede. Gradually, as the temperature increases, the network cells start to take in more water molecules and hold them within. As a result of this expansion or swelling of the cells and reduction in their flexibility, the gel starts to exhibit higher and higher elastic properties.

It may be seen that the peak of the minor curve shifted towards the right, indicating increased energy utilization with salt additives during the swelling of the gel network and the gel stabilization phase. The gradual shift of the peak to the right and the increase in the magnitude of C_{pv2} with higher NaCl concentrations may be attributed to the increasing interaction between the salt ions and water molecules that delayed the water molecules from entering the orderly state within the gel network. This is evident from Figure 4 for all the NaCl concentrations. As the salt concentration increased, higher C_{pv2} values were observed, indicating a rise in the heat energy absorbed. With additional interactions between the salt ions and the water molecules, the total enthalpy change, H_T, was higher for higher NaCl concentrations. It is evident from Figure 5 that H_T values increased linearly with NaCl concentration. The trend-line as depicted by eq. (5) shows that an additional energy of 1067.64 kJ/mol was required per 0.2*M* of NaCl.

$$H_T(\text{kJ/mol}) = 3815.7 + 5338.2 \times (\text{NaCl Concentration in } M) \quad (5)$$

However, it could not be ascertained whether the original basic energy requirement for the MC reduced in the presence of the salt.

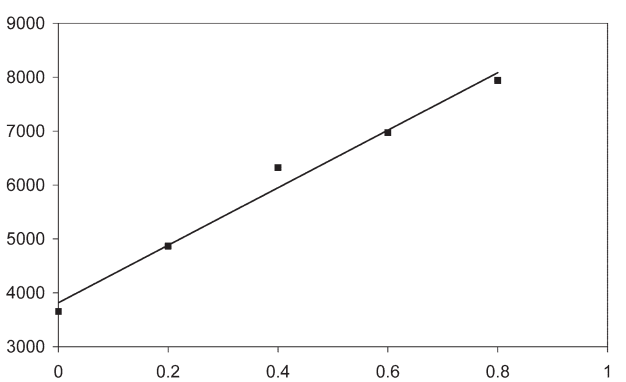

Figure 5 Total heat of gelation as a function of NaCl concentration. X axis, NaCl concentration (*M*); Y axis, total heat of gelation (kJ/mol). ■, analytical; –, linear (analytical). Equation of the line, $y = 5338.2x + 3815.7$.

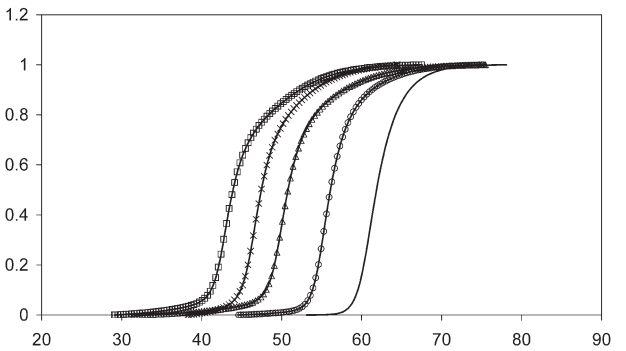

Figure 6 Degree of gelation curves for MC gelation obtained using eqs. (2) and (3). X axis, temperature (°C); Y axis, degree of gelation. –, without salt; ○, 0.2*M* of salt; △, 0.4*M* of salt; ×, 0.6*M* of salt; □, 0.8*M* of salt.

The plots of the degree of gelation versus temperature for all NaCl concentrations [determined using eq. (2)] are shown in Figure 6. The α_g curves have approximately the same slope between $\alpha_g \approx 0.1$ and 0.6. This implies that the rate of gelation was not affected by the presence of NaCl during this phase. This was the window when the MC macromolecules were moving closer and the development of the gel network was in progress.

It is evident that the formulation presented in eq. (3) could describe the energy utilization for MC gelation in the presence of NaCl. However, no specific trend for the various constants listed in Table I was observed. One of the primary reasons might be the mechanism and the transformations instigated by a specific amount of NaCl salt added to the MC solution. Although the total heat of gelation appeared to follow a linear growth with the salt concentration (Fig. 5), the internal mechanisms may not be sharing the energy in the same proportion.

Sigmoidal model for degree of gelation curves

Being a representation of a transformation process in a bio-polymeric material, the degree of gelation curves are rather similar to the degree of cure profiles for thermosetting polymers[20] and degree of crystallization curves for thermoplastics.[21] The difference is that the gelation of MC is driven predominantly by the change in temperature, and the time parameter is of little significance. As such, one could map α_g curves directly as a function of temperature instead of trying to model the rate of change in α_g. A good candidate for this purpose is the sigmoidal growth curve of the logistics curves family. It is known to describe 'S' curves well and has been used for biomedical and biomaterials related studies.[22,23] The following sigmoidal growth curve formulation [eq. (6)] was found to describe the α_g curves for gelation of MC with NaCl additive very well.

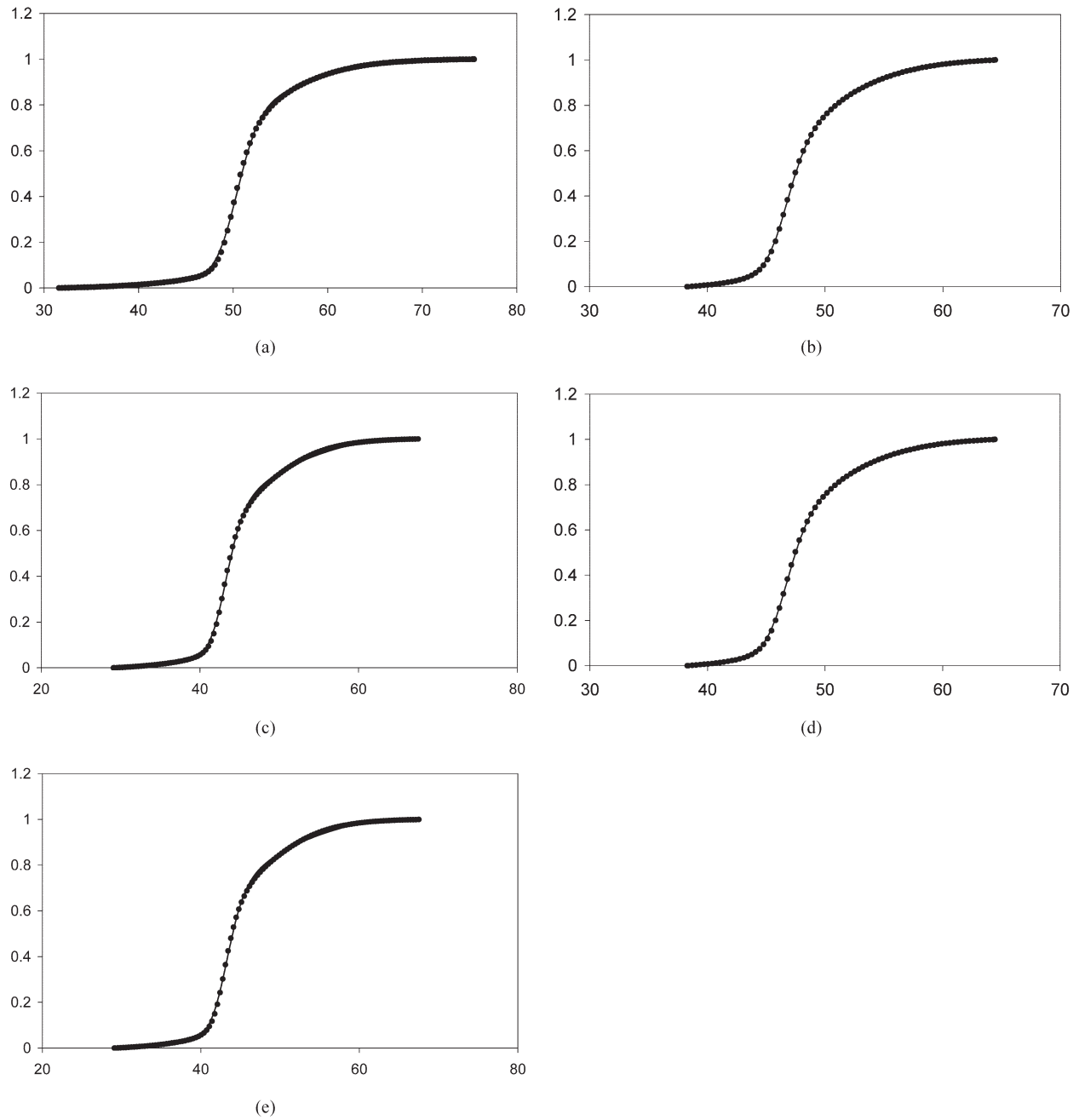

Figure 7 Plots for degree of gelation for MC hydrogels obtained using the sigmoidal model [eq. (6)]. Gelation of 0.93 wt % MC (a) without NaCl, (b) with 0.2*M*, (c) with 0.4*M*, (d) with 0.6*M*, and (e) with 0.8*M* of NaCl. X axis, temperature (°C); Y axis, degree of gelation. ●, C_p model; –, sigmoidal model.

$$\alpha_g(T - T_p) = \left(\frac{T - T_{on}}{T_{off} - T_{on}}\right)\frac{\psi_1 + \xi_1 e^{(T-T_p)B_1}}{\psi_2 + \xi_2 e^{(T-T_p)B_2}} \qquad (6)$$

Note that six empirical constants were employed in an unconstrained manner deliberately to avoid an over-constrained equation that could result in poor data fitting. $\left(\frac{T - T_{on}}{T_{off} - T_{on}}\right)$ is a temperature range fraction to enforce the limiting conditions. Similar to the $C_p(T - T_p)$ function, empirical parameters in eq. (6) are analogous to the Arrhenius terms. ξ_1 and ξ_2 are the frequency parameters and carry the unit 1/°C. ψ_1 and ψ_2 also have the same unit 1/°C. B_1 and B_2 are the activation energy parameters and their units are the same as $R/\Delta E$ terms (i.e., either 1/K or 1/°C). Thus, collectively all the numerator and denominator terms in eq. (6) bear the unit 1/°C, rendering the function $\alpha_g(T - T_p)$ nondimensionless as required.

The same least-square-error-fit procedure as discussed in Model Development and Implementation

TABLE II
The Sigmoidal Model Constants for α_g Curves [eq. (6)] and the Associated Sol–Gel Activation Energy Parameters for MC Gelation

	NaCl concentration				
Constants	0.0*M*	0.2*M*	0.4*M*	0.6*M*	0.8*M*
ψ_1 (1/°C)	—	0.0205	0.0624	0.0622	0.0702
ψ_2 (1/°C)	0.7058	0.9062	0.8654	0.5988	0.7483
ξ_1 (1/°C)	1.5502	1.5366	1.3178	1.5369	1.3668
ξ_2 (1/°C)	0.7045	0.7496	0.7303	0.7776	0.7319
B_1 (1/°C)	0.9122	0.9706	0.8125	0.9612	0.8772
B_2 (1/°C)	0.9593	1.007	0.8356	0.9999	0.9024
$\Delta E\alpha_{g1}$ (J/mol)	9.11	8.56	10.23	8.65	9.48
$\Delta E\alpha_{g2}$ (J/mol)	8.67	8.26	9.95	8.31	9.21

section was adopted to map α_g values calculated using eq. (2), based on the C_p curves modeled using eq. (3). Error minimization was achieved by employing eq. (7):

$$\sum_{i=1}^{N}[\alpha_{g(\text{ana})} - \alpha_{g(\text{sig})}]^2 \rightarrow 0 \qquad (7)$$

The results for all the cases are shown in Figure 7. A good agreement for $\alpha_{g(\text{sig})}$ was established with the analytically derived values of α_g using the C_p model (i.e., $\alpha_{g(\text{ana})}$), which was earlier found to agree well with the experimental data. The values of all the empirical constants are tabulated in Table II. It can be observed from Table II that for the no-salt case, ψ_1 term was not essential. This implied that parameter ψ_1 was associated with the salt-out effects of NaCl. Thus, the same conclusion may be reached as before that with the addition of salt, an additional mechanism is induced in the gelation process. Similar to the C_p model constants (Table I), no clear trend was observed for the sigmoid curve constants for different salt concentrations.

An attempt was made to estimate the sol–gel activation energy parameters for the degree of gelation ($\Delta E\alpha_g$) by correlating B_1 and B_2 with $R/\Delta E$ terms. The calculated $\Delta E\alpha_{g1}$ and $\Delta E\alpha_{g2}$ values, which are based on the normalized energy represented by α_g, are shown in the last two rows of Table II. These energy parameters are the process-specific remainders obtained after eliminating the effects of the process-independent universal gas constant. Thus, they relate more directly to the gelation process and the mechanism of sol–gel transformation in MC.

CONCLUSIONS

A two-bell shape model was developed for simulating the C_p curves defining heat absorption during the gelation of MC in the presence of NaCl additives. The import of various constants in terms of gelation kinetics was identified. The formulation worked well and could describe the MC gelation with different % of NaCl. Out of the two bell-shaped curves, which upon superimposing described the C_p variations with temperature, the dominant curve mapped always most of the experimental data and was designated as the primary curve. It appeared that the energy described by the curve was used mainly for the movement of MC macromolecules and their hydrophobic association, leading to the formation of a gel network. The secondary curve, which always accounted for a small amount of energy, however, was necessary to describe accurately the left and right hand shoulders of the curve. This appeared to represent the energy used in the ionic interaction of salt with water and its effects during the stabilization of the gel.

A sigmoidal model with the appropriate units for each terms was formulated to describe the degree of gelation, α_g, for all cases. The correlation between the values derived using the C_p curves and the sigmoidal model was excellent. All α_g curves had approximately the same slope, except at the beginning and towards the end of gelation. This implied that the rate of gelation was not affected by the presence of NaCl during the phase when the movement of MC chains was a dominant activity.

References

1. Peppas, N. A.; Bures, P.; Leobandung, W.; Ichikawa, H. Eur J Pharm Biopharm 2000, 50, 27.
2. Jeong, B.; Kim, S. W.; Bae, Y. H. Adv Drug Deliv Rev 2000, 54, 37.
3. Liu, W.; Zhang, B.; Lu, W. W.; Li, X.; Zhu, D.; Yao, K. D.; Wang, Q.; Zhao, C.; Wang, C. Biomaterials 2004, 25, 3005.
4. Lee, W. F.; Chiu, R. J. J Polym Res 2002, 9, 141.
5. Sarkar, N.; Walker, L. C. Carbohydr Polym 1995, 27, 177.
6. Desbrieres, J.; Hirrien, M.; Rinaudo, M. Carbohydr Polym 1998, 37, 145.
7. Ford, J. L. Int J Pharm 1999, 179, 209.
8. Kobayashi, K.; Huang, C.; Lodge, T. P. Macromolecules 1999, 32, 7070.
9. Takahashi, M.; Shimazaki, M.; Yamamoto, J. J Polym Sci Part B: Polym Phys 2001, 39, 91.

10. Joshi, S. C.; Lam, Y. C.; Li, L. In Proceedings of ANTEC 2004 Conference, Chicago, Illinois, May 16–20, 2004; p 2479.
11. Rosiak, J. M.; Yoshii, F. Nucl Instrum Methods Phys Res B 1999, 151, 56.
12. Li, L.; Shan, H.; Yue, C. Y.; Lam, Y. C.; Tam, K. C.; Hu, X. Langmuir 2002, 18, 7291.
13. Kundu, P. P.; Kundu, M. Polymer 2001, 42, 2015.
14. Xu, Y.; Wang, C.; Tam, K. C.; Li, L. Langmuir 2004, 20, 646.
15. Xu, Y. R.; Li, L.; Zheng, P. J.; Lam, Y. C.; Hu, X. Langmuir 2004, 20, 6134.
16. Lee, S. C.; Cho, Y. W.; Park, K. J Bioact Compat Polym 2005, 20, 5.
17. Lee, W. I.; Springer, G. S. J Compos Mater 1991, 25, 1632.
18. Um, M. K.; Daniel, I. M.; Hwang, B. S. Compos Sci Technol 2002, 62, 29.
19. Chang, R. Chemistry, 8th ed.; McGraw-Hill: New York, 2005; p 556.
20. Lee, W. I.; Loos, A. C.; Springer, G. S. J Compos Mater 1982, 16, 510.
21. Ozawa, T. Polymer 1977, 12, 150.
22. Rutledge, R. G. Nucleic Acids Res 2004, 32, e178.
23. DeVoe, R. D.; de Souza, J. M.; Ventura, D. F. Braz J Med Biol Res 1997, 30, 169.